Spectroscopic Investigations of Polymer Nanocomposites

*Liliane Bokobza,**[1] *Amadou Lamine Diop,*[1] *Vincent Fournier,*[1] *Jean-Baptiste Minne,*[1] *Jean-Luc Bruneel*[2]

Summary: The addition of an inorganic component to polymers leads to improvements in various physical and mechanical properties. Various examples on filled elastomeric networks will show that a mechanical characterization can be nicely combined with a spectroscopic investigation for a better understanding of the properties of the composite materials.

Introduction

In recent years nanocomposites have attracted considerable attention on account of their significant improvements in mechanical properties in comparison with pristine polymers. A wide variety of fillers have been used to reinforce polymeric materials. The efficiency of fillers to modify the properties of polymers is controlled not only by the degree of their dispersion in the host medium but also by their morphology and their interactions with the polymer matrix.[1,2]

Many synthetic routes can be used for the production of hybrid composites. In situ techniques including hydrolysis of organometallic compounds, usually generate well-dispersed filler particles (silica or titania oxide) within the polymeric matrix.[3–5] Novel reinforcing phases such as layered silicate clay minerals have generated significant research interest as a result of several examples of dramatic enhancement in mechanical, thermal and barrier properties.[6,7] The compatibility between the silicate layers and the polymer matrix is usually improved by treating the clays with ammonium cations with long alkyl chains ($R–NH_3^+$) to replace the hydrophilic Na^+ cations. This treatment renders the clays organophilic but also increases the initial interplatelet distance which favors an intercalation or an exfoliation of the clays by the polymer chains. Nanofillers with very high aspect ratio such as carbon nanotubes are expected to provide a large polymer-filler interface if a good dispersion is achieved within the matrix.[8,9] Additionally, nanocomposites based on carbon nanotubes, may display novel physical performances due to the unique mechanical and electrical properties of such fillers.

As already mentioned, the improvement in mechanical properties of polymers by the incorporation of mineral fillers, is related to interactions taking place at the polymer-filler interface. The ability of a filler to interact with macromolecular chains highly depends on its surface reactivity. On the other hand, one can expect the mobility of these chains to be strongly reduced in the vicinity of the solid surface. Several experimental techniques including molecular spectroscopies (IR, Raman, NMR) have been applied for the analysis of composites. In the present investigation, in combination with mechanical measurements, spectroscopic investigations of elastomeric materials filled with different types of fillers are reported. The aim of this work is to gain information on various aspects of filler-rubber interactions.

Experimental

Poly(dimethylsiloxane) (PDMS) composites were prepared by an in situ sol-gel

[1] Laboratoire PPMD, E.S.P.C.I., 10 Rue Vauquelin, 75231 Paris Cedex, France
E-mail: Liliane.Bokobza@espci.fr
[2] Laboratoire LPCM, Université de Bordeaux 1, 351, cours de la Libération, 33405 Talence Cedex, France

process carried out in an already-formed network. The synthesis of the unfilled PDMS network as well as the in situ filling process of silica particles were described elsewhere.[2] In brief, the polymer is cross-linked then swollen with tetraethyl orthosilicate (TEOS) which is hydrolyzed in situ. Similarly, an organo-titanate (titanium butoxide) is used to generate the inorganic phase according to the following reaction:

$$Ti[(O\,CH_2)_3CH_4] + 2H_2O \rightarrow TiO_2 + 4CH_3(CH_2)_2CH_2OH$$

The choice of this titatium alkoxide is dictated by the high reactivity of titanium ethoxide.

The composites based on hydrocarbon rubbers -natural rubber (NR) or styrene-butadiene rubber (SBR)- and clay or carbon nanotubes, were prepared as follows: appropriate quantities of filler were mixed in toluene under mechanical stirring followed by addition of the polymer and the all compounding reagents. The solvent in the resulting dispersion was carefully evaporated and the sample dried at 30 °C under vacuum. The samples were cured into plaques at 170 °C during 10 minutes under a pressure of 150 Bars.

The clay used in this study was an organomodified synthetic mica (Somasif MAE) obtained from UNICOOPJAPAN. This material consisted of agglomerated stacks of nanometer-thick silicate layers, ion exchanged with dimethyldialkyl ammonium cations.

The nanotubes (multiwall carbon nanotubes, MWNT; average outer diameter: about 10 nm; length: approximately 0.7 μm) used in the present study were obtained from Nanocyl (Belgium).

X-Ray diffraction (XRD) was used to study the nature and extent of the dispersions of the clays in the filled samples. The XDR patterns were obtained using a Philips X'Pert Pro diffractometer at the $Cu_{K\alpha}$ wavelength ($\lambda = 1.54$ Å).

The Raman spectra were recorded in the backscattering geometry on a Labram I (Jobin-Yvon, Horiba Group, France) microspectrometer in conjonction with a confocal microscope. To avoid any thermal photochemical effect, we have used a minimum intensity laser power on sample of 370 μW with the 514.5 nm incident line from an Ar-Kr laser from Spectra Physics. Detection was achieved with an air cooled CCD detector and a 1800 grooves/mm, giving a spectral resolution of 4 cm^{-1}. An acquisition time of 120 s was used for each spectrum. The confocal aperture was adjusted to 200 μm and a 50 X objective of 0.75 numerical aperture was used.

Results and Discussion

Poly(dimethylsiloxane-SiO_2 and -TiO_2 Composites

The extent of reinforcement imparted to a polymeric matrix by a filler is usually evaluated from stress-strain measurements as seen in Figure 1 for the case of poly(dimethylsiloxane) (PDMS) filled with in situ generated silica or titania oxide particles. The amount of filler is expressed in phr (parts per hundred parts of rubber). Substantial improvements in modulus and in ultimate properties (strain and deformation at break) are obtained with silica particles. Sol-gel methods have been shown to yield much smaller domains of silica and therefore greater interfacial area than conventional silica-polymer composites prepared by the usual blending process.[2] At high filler loadings and above the percolation threshold, a change in the shape of the curve is observed: the mechanical behavior is close to that of a thermoplastic polymer with a well-defined yield point followed by a smaller strain dependence of the stress. This effect is more pronounced in titania oxide-filled PDMS networks where, in addition, a reduction in extensibility is obtained. The plastics-like stress-strain curve, suggests the formation of a filler network, more developed with TiO_2 particles most probably on account of weak interfacial interactions with the elastomeric phase. An analysis by transmission electron microscopy will bring soon the necessary

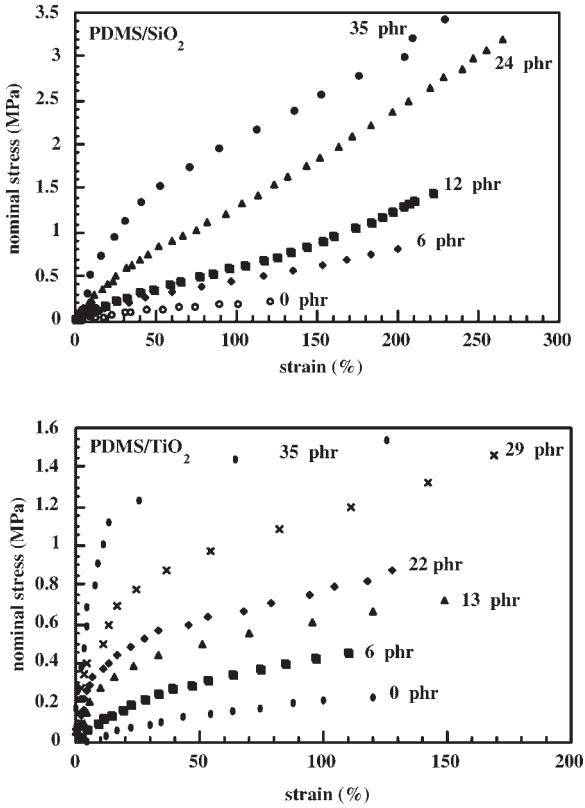

Figure 1.
Stress-strain curves of PDMS filled with in situ generated silica and titania oxide particles.

information on the difference in filler morphologies.

The rate of inorganic network formation and the final morphology of the composite are influenced by several parameters: pH, water to alkoxide ratio, catalyst, temperature and alkyl-group substitution in the alkoxide. The two precipitation reactions were run under identical conditions, in the presence of the same catalyst (dibutyltin diacetate at 3 wt%).

Infrared spectra, recorded in the near-infrared region, clearly revealed the existence of water in the PDMS/SiO_2 composites (Figure 2). The band, located around 5255 cm^{-1}, is ascribed to a combination of the bending and one of the stretching mode; it has been associated with water adsorbed on inner silanols.[10] A different water-filler interface is revealed in PDMS/TiO_2 composites (Figure 2). A spectral substraction of pure PDMS from the composites reveals a broad absorption with a maximum around 5175 cm^{-1} indicating clustering of water around the first adsorption sites.

Clay Nanocomposites

Polymer/layered clay systems can be classified into three types of composites: conventional macrocomposites, intercalated or partially exfoliated composites and fully exfoliated nanocomposites. X-ray diffraction (XRD) has been widely used for the evaluation of the degree of clay dispersion. The reinforcing effect highly depends on the state of dispersion of the silicate layers.

Figure 3 shows X-ray diffraction patterns of the pure organoclay (Somasif MAE) and of some natural rubber (NR)–clay composites. The main peak of the pure organoclay, located at 2.8° (d-spacing =

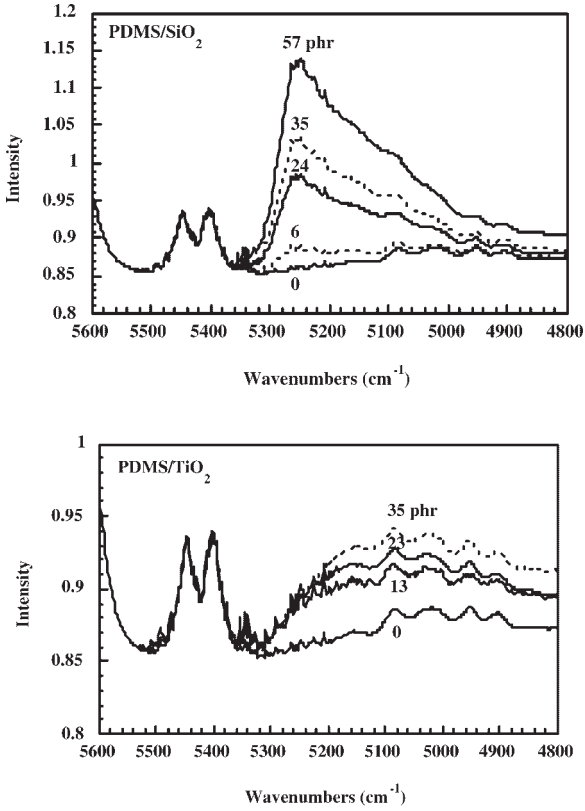

Figure 2.
Near-infrared spectra in the 4800–5600 cm^{-1} range of pure PDMS and of PDMS/SiO_2 and PDMS/TiO_2 composites. Each curve is labelled with the amount of filler in phr.

3.1 nm) is shifted around 1.6° for the sample filled with 2 phr of clay, which corresponds to an interlay spacing of approximately 5.5 nm. The results clearly reveal a pronounced intercalation of polymer chains inside the clay galleries. A further increase

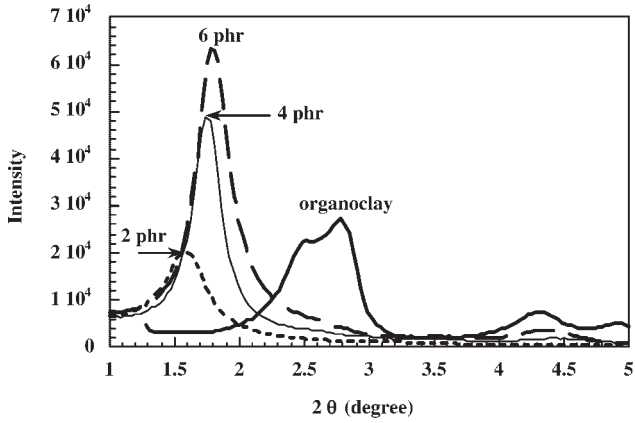

Figure 3.
X-ray diffraction patterns of organoclay (Somasif MAE) and natural rubber-organoclay composites.

Table 1.
Mechanical properties of NR and NR-clay composites.

	NR	NR-clay (2 phr)	NR-clay (4 phr)	NR-clay (8 phr)
Stress (MPa) at 100%	0.55	0.86	0.98	1.41
Stress (MPa) at 300%	1.22	1.90	2.51	3.00
Stress (MPa) at 500%	2.93	6.02	8.32	10.64

in the organoclay loading, does not improve the degree of intercalation most probably on account of a nonuniform dispersion and agglomeration.

The mechanical properties are reported in Table 1. The tensile properties are given in terms of the stresses at different strains (100, 300 and 500%). At a given strain,the stress increases with increasing filler content. For the most highly filled composite (8 phr), the stress at 500% deformation is 3.6 times greater than for the unfilled polymer.

Natural rubber is able to crystallize under strain which gives rise to a large increase in stress at high deformation. The strain-induced crystallization process is better visualized by plotting the reduced stress, σ^*, as a function of reciprocal elongation: $[\sigma^* = \sigma/(\alpha - \alpha^{-2}) = 2C_1 + 2C_2\alpha^{-1}$, where σ is the nominal stress or the force divided by the undeformed area of the sample, α is the extension ratio and $2C_1$ and $2C_2$ are constants independent of α]. Upturns in the modulus observed at high extension ratio for the unfilled as well as for the filled vulcanizates are the result of the crystallization process. The upturns occur at lower strains in the composites, showing that the organoclay favors crystallization mechanism of natural rubber (Figure 4). This observation is confirmed by infrared spectroscopy where it is seen that the band located at 837 cm^{-1} in the isotropic state, shifts to higher frequencies, upon polymer crystallization (Figure 5a). This band is associated with the C–H out-of-plane bending mode of the cis-isoprene unit. As seen in Figure 5b, the change in wavenumber upon stretching occurs at a lower extension ratio for the filled sample.

This strain-induced crystallization of natural rubber corresponds in fact to a self-toughening of the elastomer because the crystallites act as additional cross-links in the network. On the other hand, under uniaxial extension, the crystal domains are much more oriented than the polymer segments in the amorphous phase, which can explain part of the abrupt increase in the stress observed at large deformations. Measurements of chain orientation by

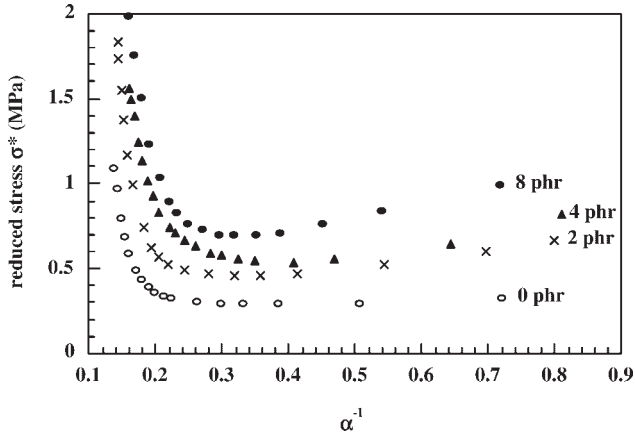

Figure 4.
Plots of reduced stress against reciprocal elongation for pure natural rubber and for composites.

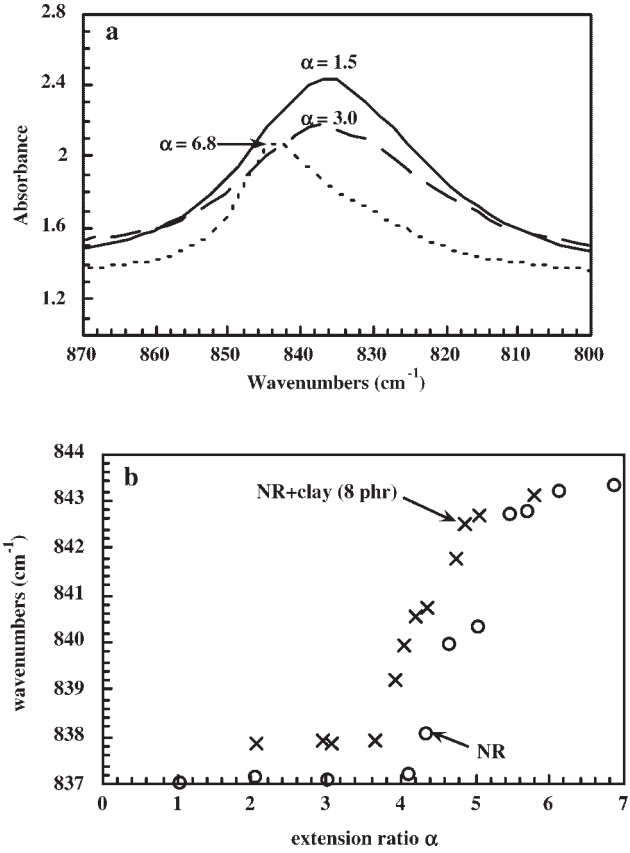

Figure 5.
Shift of the out-of-plane absorption band upon stress-induced crystallization for pure natural rubber (a) and dependence of the wavenumber of this band on the extension ratio for pure and filled polymer (b).

infrared dichroism, has revealed an increase in the orientational level of polymer segments, by addition of clay in the matrix.[11] Chain orientation under uniaxial deformation, is only sensitive to the total cross-linking density contrary to the stress-strain measurements which contain the contribution arising from the inclusion of rigid particles. So, the slope of the strain dependence of the orientation function varies as $1/M_c$ (M_c is the molecular weight between cross-links arising from chemical junctions and filler-matrix linkages). A comparison of the slope of the slopes of the orientational curves obtained for the filled and unfilled sample yield the component of the modulus ascribed to polymer-filler interactions.

Carbon Nanotube-Reinforced Elastomeric Composites

The unusual mechanical properties of carbon nanotubes make them ideal candidates as reinforcing fillers for elastomeric materials. As seen in Figure 6, in terms of mechanical stiffness improvement, 10 phr of multiwall carbon nanotubes (MWNT) impart to a styrene-butadiene rubber (SBR), a same level of reinforcement as that provided by 50 phr of carbon black.

There have been a number of promising attempts to apply Raman spectroscopy to characterize composites based on polymers filled with carbon nanotubes. Raman scattering has been used to determine morphological parameters of these nanotubes

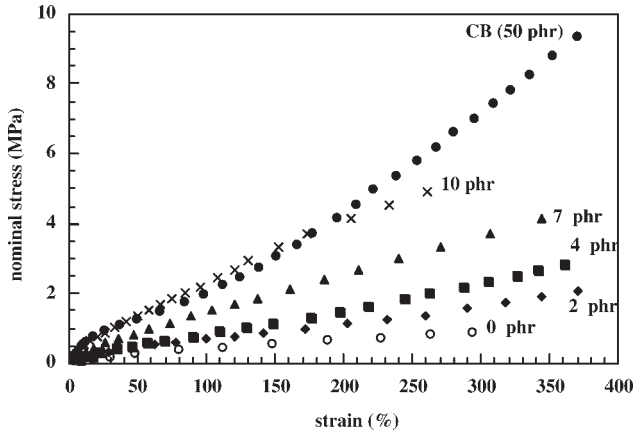

Figure 6.
Stress-strain curves of SBR/MWNT composites and of a 50 phr carbon black-filled compound.

and to characterize their interactions with the matrix.[8,12,13]

Figure 7 displays Raman spectra of pure SBR, pure MWNT and SBR/MWNT composites. With increasing the amount of nanotubes in the polymer, spectra are dominated by characteristic bands at 1347, 1598 and 2700 cm^{-1} respectively assigned to the tangential G mode, the D mode probably originating primarily from defects in the tube walls and the overtone of the D mode. Moreover, a shift toward higher frequencies ($\sim$6 cm^{-1} for the composite containing 10 phr of MWNT) is observed in the position of the D band for the nanotubes embedded in the elastomeric matrix while negligible effect is seen on the G band. Similar trends are reported for composites made on an epoxy resin and single wall carbon nanotubes (SWNT) and the shift of the D band, used to estimate the Young's modulus of carbon nanotubes, is interpreted as a compression of the C–C bonds in the nanotube shell.[14] The incorporation of SWNT in natural rubber has been shown to affect the G modes and polarization studies reveal different band position when measurements are carried out in parallel or perpendicular incident and scattered light polarization.[8] On the

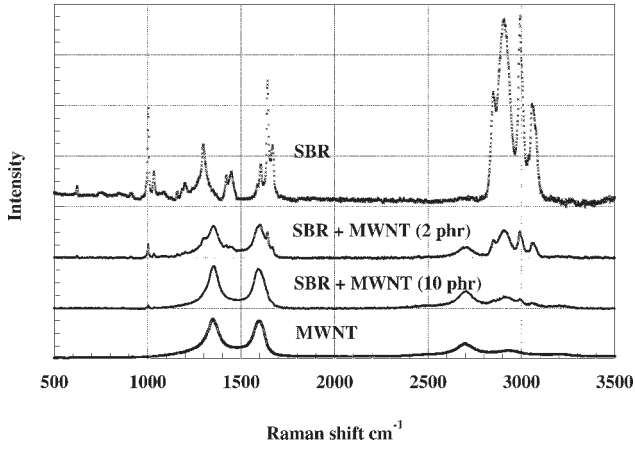

Figure 7.
Raman spectra of SBR, MWNT and MWNT/SBR composites at 514 nm excitation. Intensities of the spectra have been adjusted to improve presentation.

other hand, evidence of interfacial bonding between the polymer and the nanotubes can be obtained from the strain-induced shift of the vibrational frequency of the D* band, well known to shift with strain. Raman investigation under deformation is being investigated to determine strain sensitivity of the various modes.

These preliminary results show the potential carbon nanotubes for the design of novel, advanced composite materials. The main problem is the difficulty to obtain a homogeneous dispersion into the polymer matrix on account of th tendency of carbon nanotubes to bundle together due to Van der Waals interactions. Appropriate functionalization of carbon nanotube surface is expected, by improving the interactions with the polymer chains, to assist the dispersion and optimize the physical characteristics of the composites. There is no doubt that vibrational spectroscopy will be the appropriate tool for the characterization of the active sites on the filler surface and the interactions with the polymer chains.

[1] L. Bokobza, *Macromolecular Materials and Engineering* **2004**, *289*, 607.
[2] L. Bokobza, *Journal of Applied Polymer Science* **2004**, *93*, 2095.
[3] J. E. Mark, *Journal of Applied Polymer Science: Applied Polymer Symposium* **1992**, *50*, 273.
[4] Y. Ikeda and S. Kohjiya, *Polymer* **1997**, *38*, 4417.
[5] L. Matejka, O. Dukh and J. Kolarik, *Polymer* **2000**, *41*, 1449.
[6] M. Alexandre and P. Dubois, *Materials Science and Engineering* **2000**, *28*, 1.
[7] M. Biswas and S. Sinha Ray, *Advances in Polymer Science* **2001**, *155*, 167.
[8] M. A. López-Manchado, J. Biagiotti, L. Valentini and J. M. Kenny, *Journal of Applied Polymer Science* **2004**, *92*, 3394.
[9] F. H. Gojny, M. H. G. Wichmann, U. Köpke, B. Fiedler and K. Schulte, *Composite Science and Techology* **2004**, *64*, 2363.
[10] A. Burneau, J. P. Gallas, in: "*The Surface Properties of Silicas*", A. P. Legrand, Ed., Wiley, Chichester **1998**, p. 147–234.
[11] L. Bokobza, to be published.
[12] A. Allaoui, S. Bai, H. M. Cheng, J. B. Bai, *Composite Science and Technology* **2002**, *62*, 1993.
[13] L. Valentini, J. Biagiotti, J. M. Kenny and M. A. López-Manchado, *Journal of Applied Polymer Science* **2003**, *89*, 2657.
[14] O. Lourie and H. D. Wagner, *J. Mater. Res.* **1998**, *13*, 2418.

